Solution-Phase Synthesis of Well-Defined Indium Sulfide Nanorods

Matthew A. Franzman and Richard L. Brutchey*

Department of Chemistry and the Center for Energy Nanoscience and Technology, University of Southern California, Los Angeles, California 90089

Received January 21, 2009
Revised Manuscript Received April 6, 2009

Indium sulfide (In_2S_3), an n-type III−VI semiconductor with a midband gap ($E_g = 2.0-2.2$ eV for bulk), is currently being explored for a wide range of applications, including solar cells and phosphors for color displays.[1−8] Inorganic solar cells with In_2S_3 buffer layers were reported to have power conversion efficiencies of up to 16.4%.[4,7,9] Indium sulfide also represents a promising alternative to CdS and CdSe because it is elementally nontoxic and thermally stable, can have comparable quantum yields, and possesses a band gap in the same range as these important II−VI semiconductors.[1−4,10] Consequently, there is increasing interest in the synthesis of In_2S_3 nanocrystals and thin films. Hydrothermal,[3−5,11] solvothermal,[6,12] sonochemical,[13] and "heating-up"[2,7] methods have proven successful in the synthesis of In_2S_3; however, many of these methods require high temperatures and/or extreme pH conditions and result in products with irregular morphology.

It is known that low dimensional semiconductor nanocrystals possess size and shape dependent optoelectronic properties; strict control over morphology is therefore of critical importance when designing novel nanocrystal architectures. Large aspect ratio semiconductor nanorods possess unique electronic properties not only as a result of quantum confinement effects but also because their 1-D architecture can direct electron flow.[14,15] One dimensional $Cu_2S-In_2S_3$ heterostructures were recently reported whereby In_2S_3 grows off a 0-D Cu_2S nanocrystal in solution at 200 °C.[16] Examples of higher aspect ratio In_2S_3 nanorod syntheses are more rare, however. Room temperature sulfurization of electrodeposited metallic indium yielded 0.5-μm In_2S_3 nanorods with large diameters (>50 nm), although $In(OH)_3$ impurities were present when carried out at lower voltages.[17] Indium sulfide nanorods with lengths of 400−500 nm and diameters of approximately 20 nm were also synthesized via AACVD (aerosol-assisted chemical vapor diffusion) using a single source precursor, but this method required temperatures >375 °C to yield nanorods with good uniformity.[18]

As part of an ongoing investigation into using dialkyl dichalcogenides as low temperature chalcogen sources,[19] well-defined In_2S_3 nanorods were prepared using di-*tert*-butyl disulfide as the sulfur source in the presence of an aliphatic amine. This initial investigation describes the first example of a solution-phase synthesis of cubic β-In_2S_3 nanorods and characterization of their optoelectronic properties.

Nanorods of In_2S_3 were readily prepared by the fast injection of di-*tert*-butyl disulfide into a solution of indium acetylacetonate in oleylamine under anhydrous conditions. Nanorod formation occurred over the course of 7 h at 180 °C, resulting in a bright yellow-orange product that formed optically translucent and stable suspensions in nonpolar organic solvents, such as toluene and hexanes. An anisotropic nanorod morphology for the In_2S_3 nanocrystals (Figure 1a,b) was observed by transmission electron microscopy (TEM). The nanorods vary widely in length (mean length = 171.7 nm); however, they are quite monodisperse in diameter. Statistical analysis of approximately 300 nanorods revealed an average diameter of 11.5 ± 1.3 nm (Figure 1c), which are among the thinnest In_2S_3 nanorods reported thus far.[16] The nanocrystalline product was confirmed to be in the cubic β-phase of In_2S_3 by powder X-ray diffraction (XRD). The XRD pattern of the nanorods clearly shows the (211), (311), (222), and (440) reflections of cubic β-In_2S_3, and the general line shape and breadth of the diffraction peaks resemble those found for other anisotropic In_2S_3 nanostructures (Figure 1d).[2,4,5,20] A lattice parameter of $a = 10.7 \pm 0.3$ Å was calculated for the nanorods, which is in excellent agreement with the literature value (JCPDS no. 00-32-0456). The cubic β-phase has a defect spinel structure and remains a relatively unexplored phase of In_2S_3. X-ray photoelectron spectroscopy (XPS) was used to confirm the elemental composition of the

(1) Zhao, P.; Huang, T.; Huang, K. *J. Phys. Chem. C* **2007**, *111*, 12890.
(2) Park, K. H.; Jang, K.; Son, S. U. *Angew. Chem., Int. Ed.* **2006**, *45*, 4608.
(3) Vigneashwari, B.; Ravichandran, V.; Parameswaran, P.; Dash, S.; Tyagi, A. K. *J. Nanosci. Nanotechnol.* **2008**, *8*, 689.
(4) Chen, L.-Y.; Zhang, Z.-D.; Wang, W.-Z. *J. Phys. Chem. C* **2008**, *112*, 4117.
(5) Xing, Y.; Zhang, H.; Song, S.; Feng, J.; Lei, Y.; Zhao, L.; Li, M. *Chem. Commun.* **2008**, 1476.
(6) Naik, S. D.; Jagadale, T. C.; Apte, S. K.; Sonawane, R. S.; Kulkarni, M. V.; Patil, S. I.; Ogale, S. B.; Kale, B. B. *Chem. Phys. Lett.* **2008**, *452*, 301.
(7) Tabernor, J.; Christian, P.; O'Brien, P. *J. Mater. Chem.* **2006**, *16*, 2082.
(8) Datta, A.; Panda, S. K.; Ganguli, D.; Mishra, P.; Chaudhuri, S. *Cryst. Growth Des.* **2007**, *7*, 163.
(9) Sterner, J.; Malmstrom, J.; Stolt, L. *Prog. Photovoltaics Res. Appl.* **2005**, *13*, 179.
(10) Nagesha, D. K.; Liang, X.; Mamedov, A. A.; Gainer, G.; Eastman, M. A.; Giersig, M.; Song, J.-J.; Ni, T.; Kotov, N. A. *J. Phys. Chem. B* **2001**, *105*, 7490.
(11) Vigneashwari, B.; Dash, S.; Tyagi, A. K.; Parameswaran, P.; Ravichandran, V.; Sunthathiraraj, S. A. *J. Nanosci. Nanotechnol.* **2007**, *7*, 2087.
(12) Yu, S.-H.; Shu, L.; Wu, Y.-S.; Yang, J.; Xie, Y.; Qian, Y. T. *J. Am. Ceram. Soc.* **1999**, *82*, 457.
(13) Avivi, S.; Palchik, O.; Palchik, V.; Slifkin, M. A.; Weiss, A. M.; Gedanken, A. *Chem. Mater.* **2001**, *13*, 2195.
(14) Hu, J.; Odom, T. W.; Lieber, C. M. *Acc. Chem. Res.* **1999**, *32*, 435.
(15) El-Sayed, M. A. *Acc. Chem. Res.* **2004**, *37*, 326.
(16) Han, W.; Yi, L.; Zhao, N.; Tang, A.; Gao, M.; Tang, Z. *J. Am. Chem. Soc.* **2008**, *130*, 13152.
(17) Datta, A.; Panda, S. K.; Gorai, S.; Ganguli, D.; Chaudhuri, S. *Mater. Res. Bull.* **2008**, *43*, 983.
(18) Afzaal, M.; Malik, M. A.; O'Brien, P. *Chem. Commun.* **2004**, 334.
(19) Franzman, M. A.; Perez, V.; Brutchey, R. L. *J. Phys. Chem. C* **2009**, *113*, 630.
(20) Dutta, D. P.; Sharma, G.; Tyagi, A. K.; Kulshreshtha, S. K. *Mater. Sci. Eng., B* **2007**, *138*, 60.

10.1021/cm9002004 CCC: $40.75
Published on Web 04/15/2009

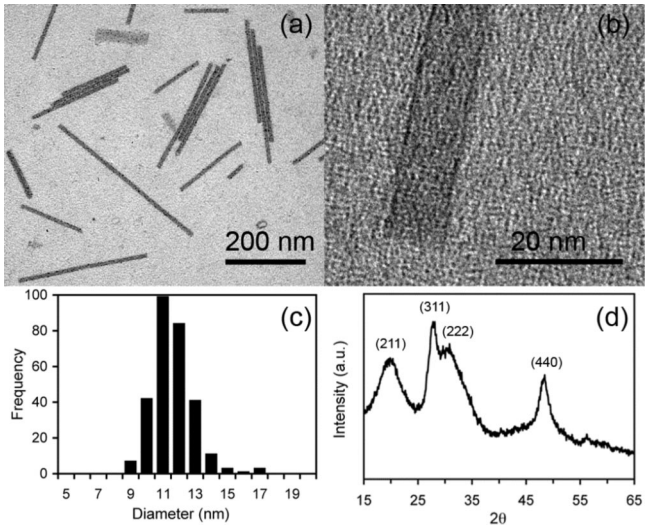

Figure 1. (a) Low-resolution TEM image of the In_2S_3 nanorods and (b) high-resolution TEM image showing the end of an isolated nanorod. (c) Size distribution of the nanorod diameter. (d) XRD pattern of the In_2S_3 nanorods.

In_2S_3 nanorods (see Supporting Information, Figure S1). Peaks at 444.7 and 452.6 eV match the reported binding energies of In $3d_{5/2}$ and In $3d_{3/2}$ for In_2S_3, respectively, and an asymmetric peak at 162.0 eV is representative of the S 2p binding energy for lattice S^{2-}.[4,21] A weak N 1s peak at 399.8 eV and a more prominent C 1s peak at 285.0 eV are assigned to the primary amine nitrogen and aliphatic carbon chain, respectively, of oleylamine bound to the surface of the purified nanorods. The surface atomic concentration was determined to be approximately 37% In and 63% S, which is close to the expected stoichiometry for In_2S_3.

In this reaction system, oleylamine (14.2 equiv based on In^{3+}) acts as both the reaction solvent and the surface pacifying ligand for the nanorods. Using stoichiometric amounts of solvent results in a high initial precursor concentration for the reaction, which has been suggested as an important variable in the formation of anisotropic nanorod structures.[22] Decreasing the initial indium acetylacetonate concentration from 0.19 to 0.10 M causes nanorods to not be formed under otherwise identical conditions. Furthermore, the concentration and type of sulfur source appear to be critical for nanorod formation. Reducing the molar equivalents of sulfur atoms from 6 to 3 (based on In^{3+}) results in the formation of mainly ill-defined particulates rather than nanorods. Moreover, adding an equimolar amount (per sulfur atom) of *tert*-butyl mercaptan instead of the disulfide produces cubic β-In_2S_3 under otherwise identical conditions; however, ill-defined nanoparticulates are formed instead of nanorods. Elemental sulfur fails to produce any crystalline products at 180 °C under these conditions. The thermal decomposition of di-*tert*-butyl disulfide begins at approximately 375 °C, which suggests that sulfur is not transferred as a result of the simple thermal decomposition of the disulfide to H_2S and 1/8 S_8.[23,24] Sulfur extraction at this

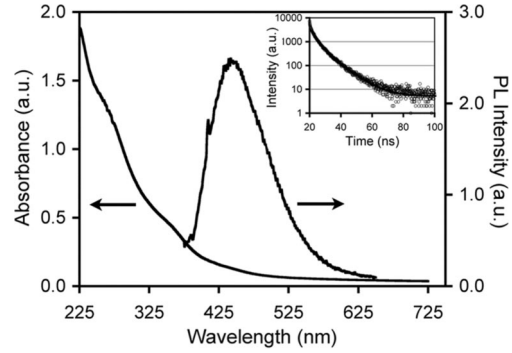

Figure 2. UV−vis absorption spectrum and steady-state photoluminescence spectrum (25 °C, λ_{ex} = 367 nm) of the In_2S_3 nanorods. The photoluminescence decay is shown as an inset (λ_{ex} = 405 nm), where the lifetime was determined in the time interval plotted.

significantly lower reaction temperature is likely facilitated by the presence of amine in the reaction mixture.[25] It is known that primary amines can react with elemental sulfur to form polysulfides and H_2S.[26,27] The oleylamine employed in this reaction may promote the S−S bond scission of di-*tert*-butyl disulfide via similar mechanisms. Together, it is the combination of high initial precursor concentrations and the use of di-*tert*-butyl disulfide as the sulfur source that provides the necessary kinetically controlled conditions for the formation of β-In_2S_3 nanorods at 180 °C.

Indium sulfide has a relatively large Bohr radius of approximately 34 nm, which is greater than the diameter of the nanorods, suggesting that quantum confinement may substantially alter the optoelectronic properties of this material.[1,3,8] The nanorods absorb strongly in the ultraviolet region of the spectrum with significant absorption in the early visible region resulting in the yellow-orange color of the product (Figure 2). Noticeable step-like contours in the absorption spectrum are observed for the valence to conduction band transition in In_2S_3.[2,3,11] The band gap of the In_2S_3 nanorods was determined from the onset of the absorption spectrum to be E_g = 2.94 eV, while bulk In_2S_3 has a reported band gap between 2.0−2.2 eV.[3−7,10] The blue-shifted band edge observed for the nanorods is indicative of quantum confinement resulting from their relatively small diameter. The steady-state photoluminescence (PL) spectrum (25 °C, λ_{ex} = 367 nm) of the In_2S_3 nanorods is given in Figure 2. The nanorods produce a single broad emission centered at λ_{max} = 445 nm (quantum yield Φ < 1%), which corresponds well with the emission characteristics of previously reported In_2S_3 nanostructures.[5,8,11] The Stokes shift of approximately 154 meV is greater than that typically observed for near band-edge emission in semiconductor nanocrystals.[28] Moreover, time-resolved PL measurements show a nonlinear decay best modeled by a double exponential fit with observed lifetimes of τ = 2.9 and 8.7 ns (α = 0.32 and 0.68, respectively; Figure 2, inset). These data suggest that the emission may be a result of trap states and/or defects in the

(21) Xiong, Y.; Xie, Y.; Du, G.; Tian, X.; Qian, Y. *J. Solid State Chem.* **2002**, *166*, 336.
(22) Peng, X. *Adv. Mater.* **2003**, *15*, 459.
(23) Bock, H.; Mohmand, S. *Angew. Chem., Int. Ed.* **1977**, *16*, 104.
(24) Martin, G.; Barroeta, N. *J. Chem. Soc., Perkin Trans. 2* **1976**, 1421.
(25) Liu, J.; Yu, H.; Wu, Z.; Wang, W.; Peng, J.; Cao, Y. *Nanotechnology* **2008**, *19*, 345602.
(26) Davis, R. E.; Nakshbendi, H. F. *J. Am. Chem. Soc.* **1962**, *84*, 2085.
(27) Mori, K.; Nakamura, Y. *J. Org. Chem.* **1971**, *36*, 3041.
(28) Zhang, J. Z. *Acc. Chem. Res.* **1997**, *30*, 423.

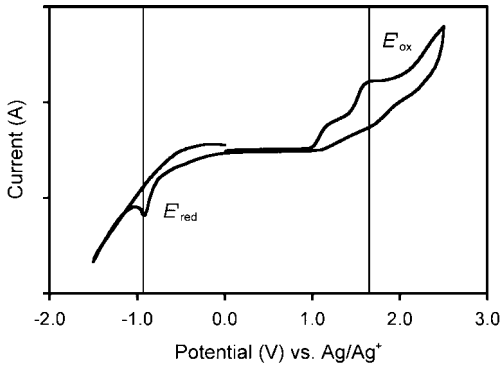

Figure 3. Cyclic voltammetry curve of the In_2S_3 nanorods (sweep rate = 10 mV s^{-1}).

In_2S_3 structure.[1,5,8] Di-*tert*-butyl disulfide is photoluminescent, but the emission profile is significantly different than the In_2S_3 nanorods (see Supporting Information, Figure S2). Oleylamine possesses a similar emission profile to that of the In_2S_3 nanorods, but much higher concentrations of oleylamine are needed to get emission at $\lambda_{ex} = 367$ nm than would be present in the purified sample of In_2S_3. Likewise, In_2O_3 nanocrystals exhibit a very weak and broad emission centered at 385 nm, ruling out the possibility that the emission observed for the In_2S_3 nanorods is a result of oxide impurities. Further investigation is needed to determine if organic surface species, or impurities from the organic species, are acting as surface trap states.

Cyclic voltammetry (CV) can be used to estimate the HOMO (valence band) and LUMO (conduction band) energies for semiconductor nanocrystals.[29,30] A typical CV curve for the In_2S_3 nanorods deposited as a thin film on the carbon working electrode is given in Figure 3. Relative to a Ag/Ag^+ reference electrode, the oxidation and reduction potentials of the nanorods are 1.64 and −0.91 V, respectively. The peak-to-peak separation between the oxidation (E'_{ox}) and reduction (E'_{red}) peaks gives an electrochemical band gap of $E_g = 2.55$ V, which is smaller than the band gap estimated from the absorption spectrum (vide supra); however, smaller electrochemical band gaps have also been measured for CdS,[30] CdSe,[31] and CdTe[32] nanocrystals. The HOMO and LUMO levels were determined to be −6.3 and −3.8 eV, respectively, as calculated from the oxidation and reduction potentials. To confirm that these oxidation and reduction peaks result from the purified nanorods and not residual di-*tert*-butyl disulfide or *tert*-butyl mercaptan byproduct, CV curves were taken with varying concentrations of disulfide added to the solution (see Supporting Information, Figure S3). As the concentration of disulfide increases, a peak at 1.88 V appears, increasing in peak current with increasing concentration. This peak is assigned to the oxidative scission of the C−S bond in the disulfide.[33] An additional peak with an onset at 1.03 V is observed in all cases; however, it can be assigned to the one electron oxidation of the disulfide to form a disulfide radical cation.[33] Furthermore, the small reduction peak at −0.91 V is not observed in the CV analysis of neat disulfide or the electrolyte blank, suggesting this peak is due to the nanorods.

In summary, we have presented a novel and facile solution-phase synthesis method that offers a pathway to very well-defined In_2S_3 nanorods at relatively low temperatures. The nanorod synthesis is based on the use of a dialkyl disulfide reagent as the sulfur source under high reaction concentrations in an aliphatic amine solvent. The resulting nanorods possess a very monodisperse diameter (11.5 ± 1.3 nm) that is well below the Bohr radius of In_2S_3, resulting in a band gap energy that is significantly blue-shifted relative to the bulk material. The band gap and HOMO and LUMO energy levels estimated for these III−VI nanorods suggest that they may be suitable alternatives to II−VI semiconductor nanocrystals in optoelectronic devices.

Acknowledgment. The authors are thankful for the generous financial support provided by the College of Letters, Arts & Sciences and the Department of Chemistry at USC. We thank Prof. M. Thompson for use of his CV, QE, and PL lifetime apparatus and Profs. M. Thompson, B. Thompson, and Dr. P. Djurovic for helpful discussions.

Supporting Information Available: Experimental details; XPS spectra; PL spectra of di-*tert*-butyl disulfide, oleylamine, and In_2O_3 nanocrystals; and CV curves of nanorods with di-*tert*-butyl disulfide (PDF). This material is available free of charge via the Internet at http://pubs.acs.org.

CM9002004

(29) Li, Y.; Zhong, H.; Li, R.; Zhou, Y.; Yang, C.; Li, Y. *Adv. Funct. Mater.* **2006**, *16*, 1705.
(30) Haram, S. K.; Quinn, B. M.; Bard, A. J. *J. Am. Chem. Soc.* **2001**, *123*, 8860.
(31) Kucur, E.; Riegler, J.; Urban, G. A.; Nann, T. *J. Chem. Phys.* **2003**, *119*, 2333.
(32) Poznyak, S. K.; Osipovich, N. P.; Shavel, A.; Talapin, D. V.; Gao, M.; Eychmuller, A.; Gaponik, N. *J. Phys. Chem. B* **2005**, *109*, 1094.
(33) Elothmani, D.; Do, Q. T.; Simonet, J.; Le Guillanton, G. *J. Chem. Soc., Chem. Commun.* **1993**, 715.